

---

ARTICLE

---

## Helium gas release behavior of highly microstructure-controlled B<sub>4</sub>C-based ceramics irradiated with helium ion beam

Katsumi Yoshida<sup>a,\*</sup>, Ryosuke Maki<sup>b</sup>, Jelena Maletaskic<sup>c</sup>, Anna Gubarevich<sup>a</sup>,  
Tatsuya Katabuchi<sup>a</sup>, Tohru S. Suzuki<sup>d</sup> and Tetsuo Uchikoshi<sup>d</sup>

<sup>a</sup>Laboratory for Zero-Carbon Energy, Institute of Innovative Research, Tokyo Institute of Technology, 2-12-1 Ookayama, Meguro-ku, Tokyo 152-8550, Japan; <sup>b</sup>Department of Applied Chemistry, Faculty of Engineering, Okayama University of Science, 1-1 Ridaicho, Kita-ku, Okayama 700-0005, Japan; <sup>c</sup>Vinca Institute of Nuclear Sciences, National Institute of the Republic of Serbia, University of Belgrade, Mike Petrovica Alasa 12-14, 11000 Belgrade, Serbia; <sup>d</sup>Research Center for Functional Materials, National Institute for Materials Science (NIMS), 1-2-1 Sengen, Tsukuba 305-0047, Japan

Boron carbide (B<sub>4</sub>C) pellets have been commonly used as neutron absorber materials in fast reactor system. In this study, highly microstructure-controlled B<sub>4</sub>C ceramics with carbon nanotube (CNT) and tubal pores were fabricated by two processes; strong magnetic field (12 T)-assisted colloidal process or normal slip casting process, and the B<sub>4</sub>C/CNT composites were irradiated with a 30-MeV alpha beam. After irradiation, the helium gas release behavior of the alpha-implanted samples was evaluated by measuring the release of helium gas by heating the samples. The alpha-implanted samples with tubal pores showed the peak which would attribute to the helium gas release clearly from around 250°C in TG-MS, whereas alpha-implanted dense sample without porosity did not show the peak clearly. It was confirmed that helium gas was released more rapidly from the B<sub>4</sub>C/CNT composites with tubal pores. The results of TG-MS and TEM suggested that helium gas can be released effectively from inside the B<sub>4</sub>C/CNT composites even with the same porosity of 5-10% as that of B<sub>4</sub>C used as neutron absorber materials in fast reactors by introducing tubal pores by highly microstructure control.

**Keywords:** boron carbide; carbon nanotube; tubal pores; helium implantation; helium gas release behavior

### 1. Introduction

Boron carbide (B<sub>4</sub>C) pellets have been commonly used as neutron absorber materials in fast reactor system because they have excellent properties such as high melting point, outstanding hardness, excellent chemical and thermal stability, light weight and high neutron absorption cross section [1].

During fast reactor operation, neutron irradiation cracks B<sub>4</sub>C pellets and fractures the pellets into pieces due to swelling, helium gas produced by the (*n*,  $\alpha$ ) reaction and thermal stress. As a result, cracks are caused in the cladding tube by the mechanical interaction induced by the swelling of B<sub>4</sub>C pellets and relocation of B<sub>4</sub>C fragments (absorber-cladding mechanical interaction (ACMI)) [2-4]. The ACMI becomes one of the reasons to limit the use period of control rods in fast reactors. Therefore, high performance B<sub>4</sub>C pellets for fast reactor system have been urgently required to extend the lifetime of control rods and to enhance the safety for fast reactor operation.

To solve these problems, the authors have paid attention to controlling microstructure of B<sub>4</sub>C ceramics with the

addition of carbon nanotubes (CNTs) to enhancing their mechanical and thermal properties. In addition, B<sub>4</sub>C pellets used as the neutron absorber materials in fast reactors contain 5-10% pores that exist independently [3,4], and the authors have proposed B<sub>4</sub>C-based ceramics that are capable of releasing helium gas by controlling the shape and orientation of pores in B<sub>4</sub>C-based ceramics with the same porosity as the B<sub>4</sub>C pellets used in fast reactors. In our attempt to develop highly microstructure controlled B<sub>4</sub>C-based ceramics with excellent mechanical and thermal properties, microstructure-controlled B<sub>4</sub>C ceramics with CNTs and highly-oriented tubal pores were successfully fabricated by strong magnetic field (12 T)-assisted colloidal process or normal slip casting process, and it is demonstrated that they showed excellent properties such as thermal conductivity and thermal shock resistance [5-9]. It has been reported that properties of B<sub>4</sub>C are anisotropic with respect to the crystallographic orientation [10], and the orientation of B<sub>4</sub>C crystals would be effective to improve its properties. B<sub>4</sub>C crystals could be highly oriented under strong magnetic field, and the mechanical and thermal properties of B<sub>4</sub>C ceramics could be improved. In addition, pores would become the structural defects, and these pores randomly existed in the ceramics would deteriorate their properties. Controlling the orientation of tubal pores is

---

\*Corresponding author. E-mail: k-yoshida@zc.iir.isct.ac.jp

considered to suppress the degradation of their properties with respect to the specific direction. To apply the B<sub>4</sub>C/CNT composites with highly-oriented tubal pores for fast reactors as the neutron absorbers, it is necessary to evaluate whether they have the capability of the release of helium gas produced by the (*n*,  $\alpha$ ) reaction or not.

In this study, microstructure-controlled B<sub>4</sub>C ceramics with CNTs and highly-oriented tubal pores were fabricated by strong magnetic field (12 T)-assisted colloidal process or normal slip casting process, and the B<sub>4</sub>C-based ceramics were irradiated with a 30-MeV alpha beam from the AVF cyclotron of the Cyclotron and Radioisotope Center (CYRIC), Tohoku University. After irradiation, the helium gas release behavior of the alpha-implanted samples was evaluated by measuring the release of helium gas by heating the samples.

## 2. Experimental procedure

### 2.1. Fabrication of highly microstructure-controlled B<sub>4</sub>C-based ceramics

In this study, highly microstructure-controlled B<sub>4</sub>C/CNT composites were prepared by strong magnetic field-assisted colloidal process or normal slip casting process. Schematic illustration of preparing quaternary aqueous suspension consisting of B<sub>4</sub>C,  $\alpha$ -Al<sub>2</sub>O<sub>3</sub>, CNT and Nylon 66 (N66) fibers used for strong magnetic field-assisted colloidal process or normal slip casting process is shown in **Figure 1**. B<sub>4</sub>C (Grade HS, average grain size; 0.8  $\mu$ m, H. C. Starck GmbH, Germany),  $\alpha$ -Al<sub>2</sub>O<sub>3</sub> (TM-D, average grain size; 0.1  $\mu$ m, Taimai Chemicals Co., Ltd., Japan) and CNT (VGCF, MWCNT, average diameter; 150 nm, average length; 5  $\mu$ m, Showa Denko K. K., Japan) were used as the starting materials. In addition, N66 fibers (for strong magnetic field-assisted colloidal process : diameter ; 10  $\mu$ m,

length ; 300  $\mu$ m; for slip casting : diameter ; 50.2  $\mu$ m, length ; 300  $\mu$ m Chubu Pile Industries, Co., Ltd., Japan) were used as pore formers. N66 fibers, B<sub>4</sub>C and  $\alpha$ -Al<sub>2</sub>O<sub>3</sub> were dispersed in distilled water with polyethyleneimine (PEI; average molecular weight; about 10000, Fujifilm Wako Pure Chemical Corporation, Japan) to improve their dispersibility. The concentration of PEI was set to 2wt% for the total amount of N66 fibers, B<sub>4</sub>C and  $\alpha$ -Al<sub>2</sub>O<sub>3</sub>. The suspension was well mixed and dispersed using a planetary centrifugal mixer (ARE-310, Thinky Corporation, Japan) at 2000 rpm for 1.5 min. CNTs were dispersed in the distilled water separately from the N66 fibers-B<sub>4</sub>C-Al<sub>2</sub>O<sub>3</sub> suspension. Then polyvinylpyrrolidone (K30, average molecular weight ; 40000, Tokyo Chemical Industry Co., Ltd., Japan) was also added to the CNT suspension to improve its dispersibility, and the suspension was well-dispersed with a planetary centrifugal mixer at 2000 rpm for 1.5 min and an ultrasonic homogenizer for 10 min. These suspensions were well-mixed with a planetary centrifugal mixer at 2000 rpm for 1.5 min and an ultrasonic homogenizer for 10 min, and then the pH of the suspension was adjusted to 6 with acetic acid (Nacalai Tesque, Inc., Japan). The composition of B<sub>4</sub>C,  $\alpha$ -Al<sub>2</sub>O<sub>3</sub> and CNT for strong magnetic field-assisted colloidal process and normal slip casting process was 85, 5 and 10vol%, and 87.5, 2.5 and 10vol%, respectively. The content of N66 fibers was 20vol% for the total amount of B<sub>4</sub>C,  $\alpha$ -Al<sub>2</sub>O<sub>3</sub> and CNT. Solid loading for the aqueous suspension was 10vol%.

In strong magnetic field-assisted colloidal process, the suspension was poured into the mold on a porous alumina plate, and the suspension was consolidated by slip casting on a turntable (1 rpm) under horizontally-applied 12 T magnetic field (JMTD-12T100, Japan Superconductor Technology, Inc., Japan). Membrane filter (pore size; 0.2

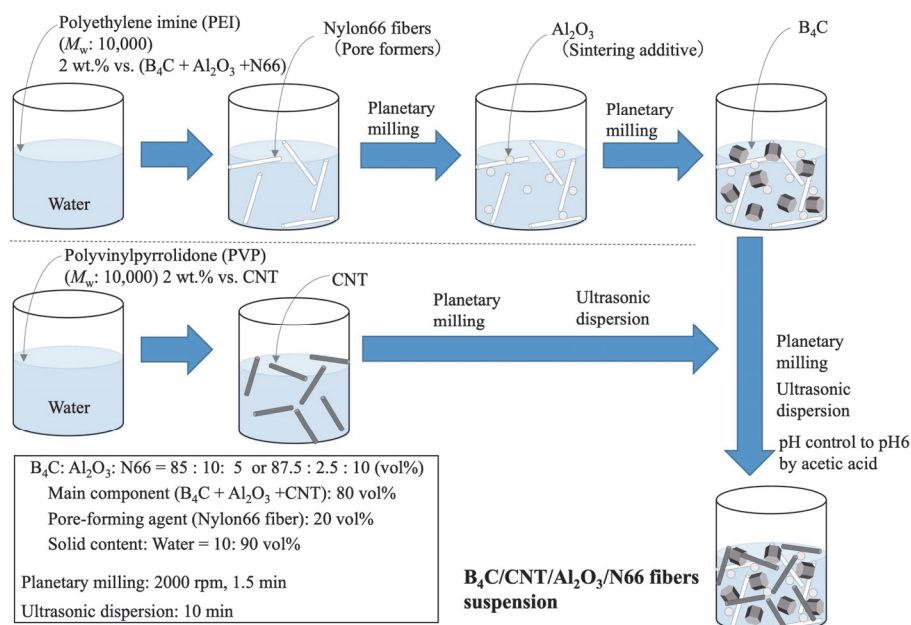


Figure 1. Schematic illustration of preparing quaternary aqueous suspension consisting of B<sub>4</sub>C,  $\alpha$ -Al<sub>2</sub>O<sub>3</sub>, CNT and Nylon 66 (N66) fibers used for strong magnetic field-assisted colloidal process or normal slip casting process.

$\mu\text{m}$ ) was inserted between the mold and porous alumina plate to control the slip casting speed. The green compacts after slip casting under a strong magnetic field were cold isostatically pressed at 392 MPa for 10 min, and then calcined at 400°C for 2 h in air to remove the N66 fibers and organic components. These compacts were spark plasma sintered (SPS, LABOX-325GH-CA, NJS Co., Ltd., Japan) at 1700°C under a uniaxial pressure of 75 MPa for 3 min in Ar flow. For comparison, dense  $\text{B}_4\text{C}/\text{CNT}$  composites without the addition of N66 fibers were also prepared.

In normal slip casting process, the suspension was poured into the mold on a porous alumina plate, and the suspension was consolidated by slip casting, and the green compacts were prepared. The compacts were cold isostatically pressed at 200 MPa for 10 min, and then calcined at 400°C for 2 h in air to remove the N66 fibers and organic components. These compacts were hot-pressed (Hi-Multi 5000, Fuji Dempa Kogyo Co., Ltd., Japan) at 2000°C under a uniaxial pressure of 40 MPa for 2 h in Ar flow. In this process, thick N66 fibers with the diameter of 50.2  $\mu\text{m}$  and the length of 300  $\mu\text{m}$  were used to avoid the closure of pores by hot-pressing.

Bulk density and porosity of the  $\text{B}_4\text{C}$ -based ceramics were measured by Archimedes' method. Crystalline phases were identified by X-ray diffractometry (XRD). Their microstructure was observed with a field-emission scanning electron microscope (FE-SEM; S-4800, Hitachi High-Tech Corporation, Japan) and an optical microscope (OM; SXH-151, Olympus Corporation, Japan).

## 2.2. Helium ion beam irradiation test and evaluation of helium gas release behavior

$\text{B}_4\text{C}/\text{CNT}$  composites were irradiated with helium ions from the 930 AVF cyclotron of CYRIC, Tohoku University. The implantation energy of helium ions was set to be 30 MeV. From calculation using the ion transport code SRIM [11], the alpha-implantation depth from the surface is 300  $\mu\text{m}$ , and this alpha-implantation depth is deep enough to evaluate whether highly controlled microstructure of  $\text{B}_4\text{C}$ -based ceramics affects helium gas release behavior or not (**Figure 2(a)**). The  $\text{B}_4\text{C}/\text{CNT}$  composite (diameter; 10 mm $\phi$ , thickness; 1 mm) was set into the sample holder as shown in **Figure 2 (b)**. The sample holder with the  $\text{B}_4\text{C}$ -based ceramics was set to the target station, and then irradiated

with 30 MeV  $\text{He}^{2+}$  beam at an average beam current around 3  $\mu\text{A}$  for 20 hours. The front surface of the sample was continually cooled with helium gas flow, and the target holder was cooled with circulating water during alpha-implantation. The release behavior of the helium existing inside the  $\text{B}_4\text{C}/\text{CNT}$  composite was evaluated with a thermogravimetry mass spectrometer (TG-MS; TG; 2020SA, Bruker AXS K.K., Japan, MS; JMS-Q1500GC, JEOL Ltd., Japan) by heating the irradiated sample from room temperature to 1000°C under argon atmosphere. The microstructure of the alpha-implanted  $\text{B}_4\text{C}/\text{CNT}$  composites was observed with a transmission electron microscope (TEM; H-9000, Hitachi High-Tech Corporation, Japan).

## 3. Results and discussion

### 3.1. Microstructure of highly microstructure-controlled $\text{B}_4\text{C}$ -based ceramics

**Figure 3** shows SEM image and schematic illustration of the microstructure of  $\text{B}_4\text{C}/\text{CNT}$  composites prepared by strong magnetic field-assisted colloidal process. SEM observation revealed that tubal pores aligned perpendicular to the applied magnetic field were well-dispersed in the  $\text{B}_4\text{C}/\text{CNT}$  composites, and this result well-agreed with Ref. [5]. The gray, black and white regions in the SEM image corresponded to  $\text{B}_4\text{C}$ , tubal pores introduced with pore formers, and segregated  $\text{Al}_2\text{O}_3$ , respectively. Average tubal pore size was around 8.6  $\mu\text{m}$ , and became slightly smaller than the diameter of N66 fibers (pore formers; 10  $\mu\text{m}$ ) due to the shrinkage caused by sintering. Porosity of the  $\text{B}_4\text{C}/\text{CNT}$  composites with/without tubal pores was 18.7% and 0.3%, respectively. From the XRD results, diffraction peak derived from (003) plane was observed as the highest peak, and the XRD result suggested that *c*-axis of  $\text{B}_4\text{C}$  particles was highly oriented in the  $\text{B}_4\text{C}/\text{CNT}$  composites perpendicular to the applied magnetic field as our previous studies reported [5,6,8]. From these results, it is demonstrated that highly microstructure-controlled  $\text{B}_4\text{C}$ -based ceramics with simultaneous orientation control of  $\text{B}_4\text{C}$  particles and tubal pores was successfully achieved.

OM image and schematic illustration of the microstructure of  $\text{B}_4\text{C}/\text{CNT}$  composites prepared by normal slip casting

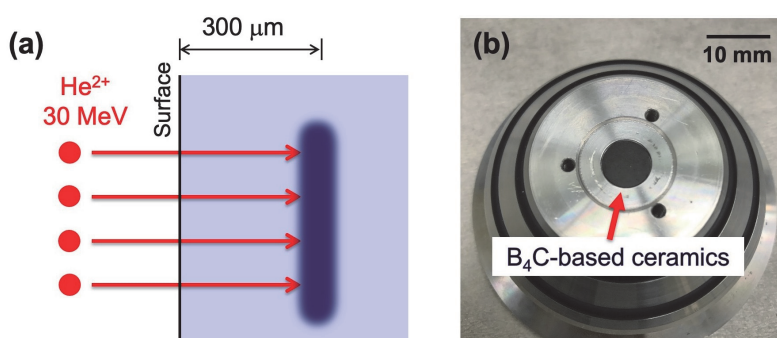


Figure 2. (a) The alpha-implantation depth from the sample surface, (b) Sample holder used for alpha-implantation.

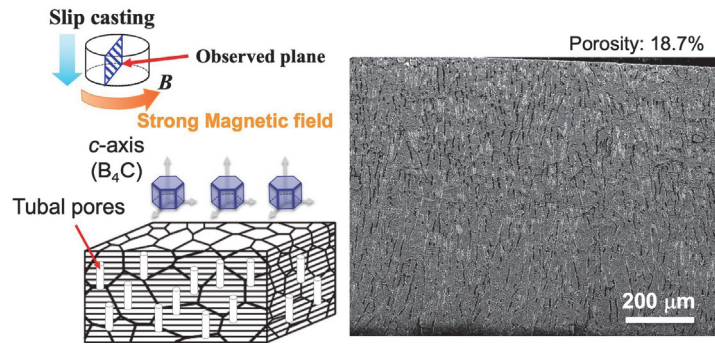


Figure 3. SEM image and schematic illustration of the microstructure of  $B_4C/CNT$  composites prepared by strong magnetic field-assisted colloidal process.

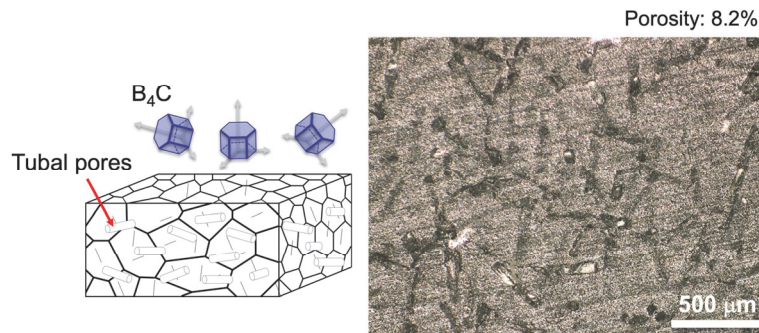


Figure 4. OM image and schematic illustration of the microstructure of  $B_4C/CNT$  composites prepared by normal slip casting process.

process is shown in **Figure 4**. Unlike the  $B_4C/CNT$  composites prepared by strong magnetic field-assisted colloidal process, tubal pores were aligned randomly in-plane of the  $B_4C/CNT$  composites. This orientation of tubal pores would be attributed to the orientation of N66 fibers (pore formers) in-plane in the  $B_4C/CNT$  composites by slip casting and the composites were prepared by hot-pressing. Average tubal pore size was about  $50 \mu m$ , almost the same as the diameter of N66 fibers, and porosity of the  $B_4C/CNT$  composites was 8.2%. This value was lower than that of the  $B_4C/CNT$  composites prepared by strong magnetic field-assisted colloidal process. The  $B_4C/CNT$  composites prepared by normal slip casting process showed that  $B_4C$  particles were randomly oriented and tubal pores were also oriented in-plane in the  $B_4C/CNT$  composites.

### 3.2. Helium gas release behavior of highly microstructure-controlled $B_4C$ -based ceramics

Porosity, composition, fabrication process of  $B_4C/CNT$  composites and helium ion fluence in helium ion beam irradiation test are listed in **Table 1**. Hereafter the  $B_4C/CNT$  composites with/without tubal pores prepared by strong magnetic field-assisted colloidal process and the composites prepared by normal slip casting process are denoted as sample A, sample B and sample C, respectively. Helium ion fluence for sample A, B and C was  $7.67 \times 10^{17}$ ,  $6.20 \times 10^{17}$  and  $8.03 \times 10^{17}$  ion/cm<sup>2</sup>, respectively.

**Figure 5** shows mass chromatograph (helium,  $m/z=4$ ) of alpha-implanted  $B_4C/CNT$  composites prepared by strong magnetic field-assisted colloidal process (sample A and B) and un-implanted composite (blank sample) by TG-MS. In the case of un-implanted sample (blank sample), the peak did not appear in the mass chromatograph during heating from room temperature to  $1000^\circ C$ , and this result indicated that helium was not released from the un-implanted sample. On the other hand, helium gas was

Table 1. Porosity, composition, fabrication process of  $B_4C/CNT$  composites and helium ion fluence in helium ion beam irradiation test.

Sample	A	B	C
Fluence (ion/cm <sup>2</sup> )	$7.67 \times 10^{17}$	$6.20 \times 10^{17}$	$8.03 \times 10^{17}$
Porosity (%)	0.3	18.7	8.2
Sample composition (vol%)	85% $B_4C$ /5% $Al_2O_3$ /10% CNT		87.5% $B_4C$ /2.5% $Al_2O_3$ /10% CNT
Fabrication process	Strong magnetic field-assisted colloidal process and spark plasma sintering		Normal slip casting process and hot-pressing

released from both alpha-implanted samples (A and B) in the temperature region of 250-400°C. However dense sample without porosity (sample A, porosity: 0.3%) showed the gradual and slight increase of the peak in the temperature region of 250-400°C, and clear peak was not observed. This result indicated that the amount of helium gas release from the sample was very small. On the other hand, the peak was clearly observed in the temperature region of 250-400°C for the porous sample (sample B, porosity: 18.7%), and it was confirmed that helium gas was released more rapidly from sample B (porous) than from sample A (dense), and tubal pores would be effective to release helium gas from the B<sub>4</sub>C/CNT composites.

The microstructure change of the B<sub>4</sub>C/CNT composites by helium ion beam irradiation was evaluated by TEM. **Figure 6** shows TEM images of un-implanted and as-

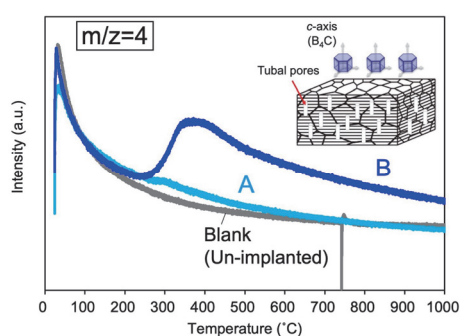


Figure 5. Mass chromatograph (He,  $m/z=4$ ) of alpha-implanted B<sub>4</sub>C/CNT composites with/without tubal pores (sample A; without tubal pores, sample B; with tubal pores) prepared by strong magnetic field-assisted colloidal process and blank sample (un-implanted) by TG-MS.

alpha-implanted B<sub>4</sub>C/CNT composites with tubal pores. B<sub>4</sub>C grains, grain boundaries and CNT in the B<sub>4</sub>C/CNT composites from the helium ion beam irradiated surface to a region of 300 μm were observed by TEM. Helium bubbles were not observed in either B<sub>4</sub>C grains, grain boundaries or CNT in the as-alpha-implanted B<sub>4</sub>C/CNT composites, and the difference between the un-implanted and alpha-implanted samples was not observed clearly.

Alpha-implanted B<sub>4</sub>C/CNT composites after heating were observed by TEM to evaluate their microstructure change with heating. TEM image of alpha-implanted B<sub>4</sub>C/CNT composites with tubal pores after heating at 1000°C was shown in **Figure 7**. Helium bubbles with the diameter of around 10-50 nm were clearly observed inside B<sub>4</sub>C grains (helium bubbles are indicated with arrows in this image). This result indicated that helium ion implanted into the B<sub>4</sub>C/CNT composites diffused and grew into helium bubbles with heating. These helium bubbles were observed only inside B<sub>4</sub>C grains, and not observed at grain boundaries.

To understand the effect of heat-treatment temperature on the formation of helium bubbles, microstructure change of the alpha-implanted B<sub>4</sub>C/CNT composites with tubal pores after heating at 800°C and 1300°C were also observed by TEM. **Figures 8 and 9** shows TEM images of alpha-implanted B<sub>4</sub>C/CNT composites with tubal pores after heating at 800°C and 1300°C, respectively. Circular defects, which would be considered to be helium bubbles with the size of around 50 nm in diameter, were observed in B<sub>4</sub>C grain at a depth of 300 μm from the surface, and these bubbles were not observed near the surface of the sample. On the other hand, helium bubbles were observed even near the surface of the alpha-implanted B<sub>4</sub>C/CNT

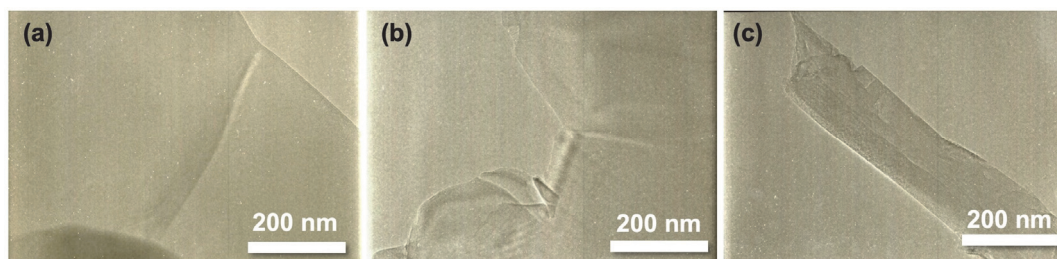


Figure 6. TEM images of (a) un-implanted, (b) B<sub>4</sub>C particles and (c) CNT in as-alpha-implanted B<sub>4</sub>C/CNT composites with tubal pores prepared by strong magnetic field-assisted colloidal process.

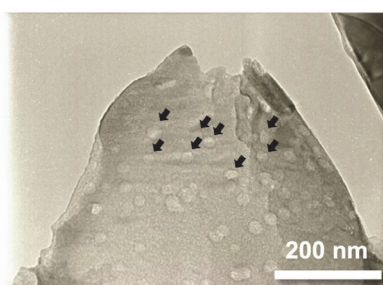


Figure 7. TEM image of helium bubbles (indicated with arrows) inside the alpha-implanted B<sub>4</sub>C/CNT composites with tubal pores after heating at 1000°C.

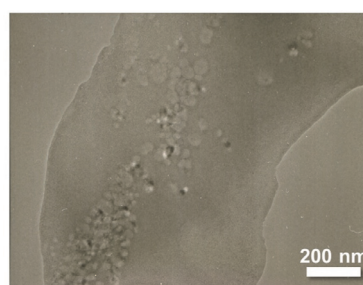


Figure 8. TEM image of helium bubbles inside the alpha-implanted B<sub>4</sub>C/CNT composites with tubal pores after heating at 800°C.

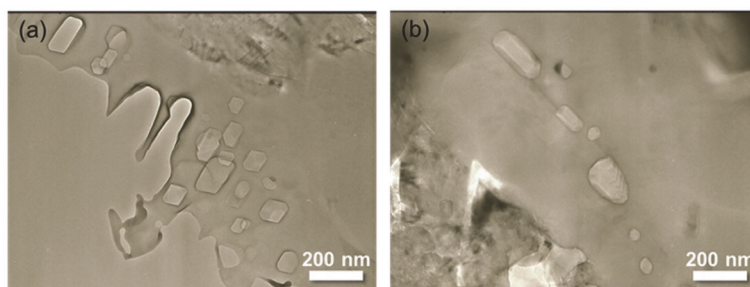


Figure 9. TEM image of helium bubbles inside the alpha-implanted  $B_4C/CNT$  composites with tubal pores after heating at  $1300^\circ C$ . (a) inside  $B_4C$  particle and (b) along grain boundary.

composites after heating at  $1300^\circ C$  as shown in Figure 9 (a). Furthermore helium bubbles grown significantly to the size of around 100 nm overlapped together existed at a depth of around  $300\ \mu m$  from the surface, and the trace of the release of helium bubbles to the pores were observed. These helium bubbles were thought to grow in a certain direction along the specific crystal plane [111] of  $B_4C$  [12,13], and thus the bubbles had polygonal shapes. This growth behavior of helium bubbles was very similar to that of neutron-irradiated  $B_4C$  used as control rod materials, and it is confirmed that the present experimental procedures using helium ion beam irradiation would be validated to simulate the formation and diffusion of helium bubbles in the  $B_4C/CNT$  composites. Similarly, He bubbles grown preferentially in a certain direction were also observed at the grain boundaries as shown in Figure 9 (b).

Figure 10 shows mass chromatograph (helium,  $m/z=4$ ) of alpha-implanted  $B_4C/CNT$  composites prepared by normal slip casting process (sample C) by TG-MS. Peak which would attribute to helium gas release appeared around  $300^\circ C$ , and this result indicated that the release of helium gas from inside the sample even with the porosity of 8.2% was promoted effectively. Furthermore, it is found that the introduction of tubal pores to the  $B_4C/CNT$  composites would be important for the release of helium gas regardless of the orientation of  $B_4C$  crystals.

From these results, it is concluded that helium gas can be released effectively from inside the  $B_4C/CNT$  composites even with the same porosity of 5-10% as that of  $B_4C$  used as control rod materials for fast reactors by introducing tubal pores by highly microstructure control.

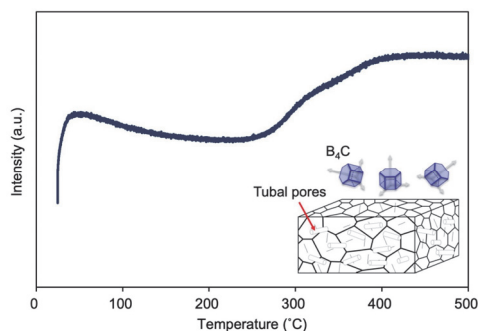


Figure 10. Mass chromatograph (He,  $m/z=4$ ) of alpha-implanted  $B_4C/CNT$  composites with tubal pores fabricated by normal slip casting by TG-MS.

#### 4. Conclusion

In this study, highly microstructure-controlled  $B_4C$  ceramics with CNT and tubal pores was fabricated by two processes; strong magnetic field (12 T)-assisted colloidal process or normal slip casting process, and the  $B_4C/CNT$  composites were irradiated with a 30-MeV alpha beam. After irradiation, the He gas release behavior of the alpha-implanted samples was evaluated by measuring the release of helium gas by heating the samples. Both alpha-implanted  $B_4C/CNT$  composites with tubal pores prepared by strong magnetic field-assisted colloidal process or normal slip casting process showed the peak which would attribute to the helium gas release clearly from around  $250^\circ C$ , and it is found that the introduction of tubal pores to the  $B_4C/CNT$  composites would be important for the release of helium gas regardless of the orientation of  $B_4C$  crystals. In addition, TEM observation revealed that the growth behavior of helium bubbles was very similar to that of neutron-irradiated  $B_4C$  used as control rod materials, and it is confirmed that the present experimental procedures using He ion beam irradiation would be validated to simulate the formation and diffusion of He bubbles in the  $B_4C/CNT$  composites.

In conclusion, these results suggested that helium gas can be released effectively from inside the  $B_4C/CNT$  composites even with the same porosity of 5-10% as that of  $B_4C$  used as control rod materials for fast reactors by introducing tubal pores by highly microstructure control.

#### Acknowledgements

This work was partially supported by The Ministry of Education, Culture, Sports, Science and Technology (MEXT) under the framework of Innovative Nuclear Research and Development Program.

#### References

- [1] F. Thevenot, Boron Carbide-A Comprehensive Review, *J. Eur. Ceram. Soc.*, 6 (1990), pp. 205-225.
- [2] T. Donomae, K. Katsuyama, Y. Tachi, K. Maeda, M. Yamamoto and T. Soga, Reduction in Degree of Absorber-Cladding Mechanical Interaction by Shroud Tube in Control Rods for the Fast Reactor, *J. Nucl. Sci. Tech.* 48 (2011), pp. 580-584.
- [3] T. Donomae and K. Maeda, Fast Spectrum Control Rod Materials, in: Konings, R.J.M., Allen, T.R., Stoller, R.E., Yamanaka, S. (Eds), *Comprehensive*

- Nuclear Materials Volume 3 Advanced Fuels/Fuel Cladding/Nuclear Fuel Performance Modeling and Simulation*. Elsevier, The Netherlands, (2012), pp. 509-534.
- [4] S. Sasaki, K. Maeda and H. Furuya, Irradiation Performance of Sodium-Bonded Control Rod for the Fast Breeder Reactor, *J. Nucl. Sci. Tech.* 55 (2018), pp. 276-282.
- [5] S. Azuma, T. Uchikoshi, K. Yoshida and T.S. Suzuki, Preparation of textured B<sub>4</sub>C compact with oriented pore-forming agent by slip casting under strong magnetic field, *J. Ceram. Soc. Japan* 126 (2018), pp. 832-838.
- [6] M. Fajar, A. Gubarevich, R.S.S. Maki, T. Uchikoshi, T.S. Suzuki, T. Yano and K. Yoshida, Effect of Al<sub>2</sub>O<sub>3</sub> addition on texturing in a rotating strong magnetic field and densification of B<sub>4</sub>C, *Ceram. Int.* 45 (2019), pp. 18222-18228.
- [7] R.S.S. Maki, M. Fajar, J. Maletaskic A.V., Gubarevich, K. Yoshida, T. Yano, T.S. Suzuki and T. Uchikoshi, Evaluation of thermal shock fracture resistance of B<sub>4</sub>C/CNT composites with a high-frequency induction-heating furnace, *Mater. Today; Proc.* 16 (2019), pp. 137-143.
- [8] S. Azuma, T. Uchikoshi, K. Yoshida and T.S. Suzuki, Fabrication of textured B<sub>4</sub>C ceramics with oriented tubal pores by strong magnetic field-assisted colloidal processing, *J. Eur. Ceram. Soc.* 41 (2021), pp. 2366-2374.
- [9] R.S.S. Maki, M. Fajar, J. Maletaskic, A.V. Gubarevich, K. Yoshida, T. Yano, T.S. Suzuki and T. Uchikoshi, Effect of CNT addition and its orientation on thermal shock resistance of B<sub>4</sub>C/CNT composites fabricated by hot-pressing, *J. Asian Ceram. Soc.* 10 (2022), pp. 370-377.
- [10] S. Grasso, C. Hu, O. Vasylykiv, T.S. Suzuki, S. Guo, T. Nishimura and Y. Sakka, High-hardness B<sub>4</sub>C textured by a strong magnetic field technique, *Scr. Mater.* 64 (2011), pp. 256-259.
- [11] J.F. Ziegler, M.D. Ziegler and J.P. Biersack, SRIM—The stopping and range of ions in matter, *Nucl. Instrum. Meth. B* 268 (2010), pp. 1818-1823.
- [12] T. Donomae, Y. Tachi, M. Sekine, Y. Morohashi, N. Akasaka and S. Onose, Neutron irradiation effects on <sup>11</sup>B<sub>4</sub>C and recovery by annealing, *J. Ceram. Soc. Japan* 115 (2007), pp. 551-555 [Japanese].
- [13] Y. You, K. Yoshida, T. Inoue and T. Yano, Helium bubbles and trace of lithium in B<sub>4</sub>C control rod pellets used in JOYO experimental fast reactor, *J. Nucl. Sci. Technol.* 55 (2018), pp. 640-648.
-